J. Phys. Chem. A **2004,** *108,* 10789−10793

Electronic Spectra of Jet-Cooled 3-Methyl-7-azaindole Dimer. Symmetry of the Lowest Excited Electronic State and Double-Proton Transfer

Akihiko Hara,† Yusuke Komoto,† Kenji Sakota,† Riko Miyoshi,† Yoshiya Inokuchi,‡ Kazuhiko Ohashi,† Kanji Kubo,§ Emi Yamamoto,§ Akira Mori,§ Nobuyuki Nishi,‡ and Hiroshi Sekiya*,†

Department of Molecular Chemistry, Graduate School of Science, and Department of Chemistry, Faculty of Sciences, Kyushu University, 6-10-1 Hakozaki, Higashi-ku, Fukuoka 812-8581, Japan, Institute for Molecular Science, Myodaiji, Okazaki,444-8585, Japan, and Institute for Material Chemistry and Engineering, Kyushu University, 6-1 Kasuga-Koen, Kasuga 816-8580, Japan

Received: August 2, 2004; In Final Form: September 17, 2004

The fluorescence excitation spectra are recorded for jet-cooled dual hydrogen-bonded 3-methyl-7-azaindole dimer $(3MAI)_2$-*hh* and deuterated dimers $(3MAI)_2$-*hd* and $(3MAI)_2$-*dd* near the electronic origin region of the S_1-S_0 transition, where *hd* and *dd* indicate the deuteration of an imino hydrogen and two imino hydrogens, respectively. A single origin is detected in the spectra of $(3MAI)_2$-*hh* and $(3MAI)_2$-*dd*, whereas two electronic origins separated by 13 cm^{-1} are detected in the spectrum of $(3MAI)_2$-*hd*. The excited-state double-proton transfer (ESDPT) occurs in $(3MAI)_2$-*hh*, while $(3MAI)_2$-*hd* and $(3MAI)_2$-*dd* undergo excited-state proton/deuteron transfer and excited-state double deuteron transfer, respectively. In $(3MAI)_2$-*hd*, the excitation is localized on either the 3MAI-*h* or 3MAI-*d* moiety. The localization of the excitation is explained by a weak coupling of the excitonic states of $(3MAI)_2$-*hh* and $(3MAI)_2$-*dd*. The effective symmetry of the lowest excited state of $(3MAI)_2$-*hh* and $(3MAI)_2$-*dd* belongs to the C_{2h} point group, while that of $(3MAI)_2$-*hd* belongs to the C_s point group. The vibronic patterns in the excitation spectra of the $(3MAI)_2$ dimers is very similar to those of the 7-azaindole dimers, indicating that the methyl substitution provides little effect on the shape of the ESDPT potential.

1. Introduction

Dual hydrogen-bonded complexes such as the 7-azaindole dimer $(7AI)_2$,[1−13] the 2-pyridone/2-hydroxypyridine dimer,[14] and the 2-aminopyridine dimer[15] have been of considerable interest in the excited-state double-proton transfer (ESDPT) reaction.[14] These complexes are considered as model systems of the DNA base pairs. Among various dual hydrogen-bonded dimers, $(7AI)_2$ is the most extensively studied molecule. Steady-state and time-resolved studies showed that the ESDPT reaction occurs in $(7AI)_2$ that has a planar double hydrogen-bonded structure.[1−13] The mechanism of the ESDPT reaction has been a subject of experimental and theoretical studies. In the stepwise mechanism, ESDPT occurs sequentially via an intermediate state, but two protons transfer simultaneously in the concerted mechanism.[3]

The observation of biexponential decay profiles in the femtosecond time-resolved transients of $(7AI)_2$ ions in a molecular beam was attributed to a decay from a photoexcited initial state to a single-proton-transferred intermediate state, and that from the intermediate state to the double-proton-transferred tautomer state.[3] Essentially the same conclusion was derived from a femtosecond time-resolved study with the Coulomb explosion technique.[7] However, very recently, we measured the UV−UV hole-burning spectra of $(7AI)_2$-*hh*, $(7AI)_2$-*hd*, and $(7AI)_2$-*dd*. The analysis of the spectra shows that the biexponential decay profiles observed by Douhal et al.[3] are due to simultaneous excitation of vibronic states that have long and short decay times. The difference in the decay times originates from vibrational-mode selective ESDPT: The intermolecular stretching vibration enhances ESDPT, but the intermolecular bending vibration suppresses it. Our results indicate that the observation of the biexponential decay profiles in the femtosecond transients cannot be direct evidence for the stepwise mechanism.

The excitonic character of the lowest excited state should be taken into account to investigate the ESDPT dynamics in $(7AI)_2$, because the initial state of the reaction may determine the ESDPT reaction process. We showed that the excitation is delocalized on the two monomer moieties in $(7AI)_2$-*hh* and $(7AI)_2$-*dd*, but it is localized on either the 7AI-*h* or 7AI-*d* moiety in $(7AI)_2$-*hd*. The investigation of the deuterated dimers provides information on the symmetry of the excited state of the dual hydrogen-bonded dimers.[12]

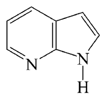

7AI

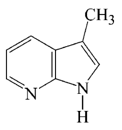

3MAI

The substitution of an electron-donating or an electron-withdrawing group in a CH hydrogen of the indole ring may change the strength of the intermolecular hydrogen bond and the ESDPT potential of $(7AI)_2$. The ESDPT reaction in substituted $(7AI)_2$ dimers has been studied in the condensed

---

* To whom correspondence should be addressed. E-mail: hsekiscc@mbox.nc.kyushu-u.ac.jp.

† Department of Chemistry, Kyushu University.

‡ Institute for Molecular Science.

§ Institute of Material and Engineering Sciences, Kyushu University.

10.1021/jp0465480 CCC: $27.50

phase by electronic spectroscopy,[16−18] but no report has been presented about the electronic spectra of the substituted $(7AI)_2$ dimers in the gas phase. Thus, we have investigated ESDPT in a 3-methyl-7-azaindole dimer $(3MAI)_2$ and its deuterated species. Yu et al. studied the ESDPT reaction in 3MAI in a single crystal.[18] They remarked that 3MAI was a good model system to investigate ESDPT in a crystal, because ESDPT does not occur in a 7AI crystal because of the absence of the dual hydrogen-bonded structure. However, information on the vibronic states, which is very important for a discussion of the mechanism of ESDPT, cannot not be obtained from the electronic spectrum of $(3MAI)_2$ in a single crystal. The observation of the electronic spectrum of $(3MAI)_2$ under the jet-cooled conditions promises to provide more detailed information on the symmetry of the dimer in the excited electronic state and the vibrational-mode selective ESDPT. We discuss the effects of the substitution of a methyl group and deuteration of the imino proton on the ESDPT reaction by measuring the laser-induced fluorescence (LIF) spectra of jet-cooled $(3MAI)_2$-*hh*, $(3MAI)_2$-*hd*, and $(3MAI)_2$-*dd* and performing density functional theory (DFT) calculations of the geometry and intermolecular vibrational modes.

2. Experimental Section

3MAI was synthesized following a method in the literature.[19] The melting point of the sample (131.5−133 °C) and elementary analysis data (C,72.78; H, 6.07; N, 21.29 calculated for $C_8H_8N_2$: C, 72.70; H, 6.10; N, 21.20) were in good agreement with reported values.[18] The experimental apparatus for the measurement of LIF and dispersed fluorescence spectra was essentially the same as that reported previously.[14] Briefly, the 3MAI vapor was prepared by heating the solid 3MAI sample to 80−100 °C. A gas mixture of 3MAI and helium was expanded into a vacuum chamber with a pulsed nozzle (General Valve series 9, 0.5-mm orifice diameter). The backing pressure was 200 kPa. The 3MAI molecules were excited by an Nd:YAG laser pumped-dye laser system (Spectra Physics GCR230 and HD-300). The output of the dye laser was frequency-doubled in a KDP crystal. The LIF spectra were measured by monitoring total fluorescence with a photomultiplier tube (Hamamatsu 1P28A). Dispersed fluorescence spectra were measured with a monochromator (Spex 1704) equipped with a photomultiplier tube (Hamamatsu R955). The electric current from the photomultiplier tubes was fed into a digital oscilloscope (LeCroy 9310A) and processed by a PC.

Structures of $(3MAI)_2$ were optimized by DFT calculations at the B3LYP/cc-pVDZ level with a *Gaussian 98* program package.[20] The total energies and binding energies were calculated with the correction of the zero-point energy (ZPE) and the basis set superposition error (BSSE). Normal-mode calculations were made to assign vibronic bands detected in the LIF spectrum.

3. Results and Discussion

3.1. LIF Spectra of a Reactive Dimer. We observed an LIF spectrum of jet-cooled 3MAI in the 33 200−35 100 cm^{-1} region (Figure 1). The strongest band at 33 432 cm^{-1} in Figure 1 was assigned to the origin of the $S_1 \leftarrow S_0$ ($\pi-\pi^*$) transition of the 3MAI monomer. In the lower wavenumber region of the LIF spectrum of the 3MAI monomer, a new transition system has been observed, as shown in Figure 2, where a Toshiba Y45 cutoff filer is used to detect only largely red-shifted fluorescence (λ > 420 nm) from the excitation wavelength. The vibronic pattern in Figure 2 is very similar to that in the LIF spectrum of $(7AI)_2$-*hh*, and the bandwidth remarkably depends on the vibronic state. These findings indicate that a vibrational-mode selective fast decay process occurs after photoexcitation. Thus, this new system in Figure 2 has been assigned to the transition from the S_0 state to the lowest excited electronic state of a $(3MAI)_2$-*hh* dual hydrogen-bonded dimer, and the fast decay process must be the ESDPT reaction. The observation of ESDPT is consistent with the result in a single crystal.[18]

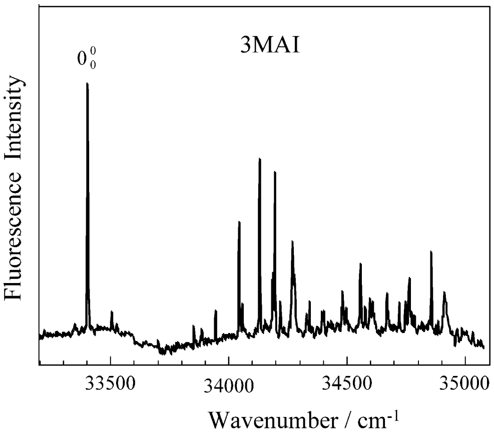

Figure 1. The S_1-S_0 ($\pi-\pi^*$) fluorescence excitation spectrum of jet-cooled 3MAI monomer in the 33 400−35 000 cm^{-1} region. The origin band is observed at 33 432 cm^{-1}.

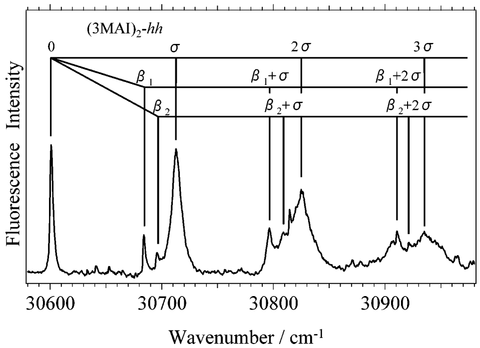

Figure 2. The LIF spectrum of jet-cooled $(3MAI)_2$-*hh* in the 31 700−33 400 cm^{-1} region. A Toshiba Y45 glass filter is used to detect the red-shifted fluorescence. The spectrum has been assigned to the $^1B_u-{}^1A_g$ ($\pi-\pi^*$) transition of $(3MAI)_2$-*hh* (see the text).

The electronic origin band of $(3MAI)_2$-*hh* is detected at 30 600 cm^{-1}, which is 2832 cm^{-1} red-shifted from that of the 3MAI monomer. The assignment of vibronic bands is made by comparing the vibronic pattern in the spectrum of $(3MAI)_2$-*hh* with that of $(7AI)_2$-*hh* together with DFT calculations of the intermolecular vibrational modes, which will be shown in Section 3.2. Prominent vibronic bands in Figure 2 are assigned to the intermolecular stretching vibration (σ), intermolecular bending vibrations β_1 and β_2, and their combinations.

Figure 3 displays the LIF spectrum of a mixture of undeuterated and deuterated $(3MAI)_2$ dimers. We have assigned the vibronic bands of $(3MAI)_2$-*hd* and (3MAI)-*dd* by comparing the vibronic pattern in Figure 3 with that in the LIF spectra of $(7AI)_2$-*hh*.[2,12] Two electronic origin bands are observed at 30 641 and 30 655 cm^{-1} in $(3MAI)_2$-*hd*, while an electronic origin band of $(7AI)_2$-*dd* is observed at 30 691 cm^{-1}. The wavenumbers, the bandwidths (fwhm), and the assignment for vibronic bands in the LIF spectra of $(3MAI)_2$-*hh*, $(3MAI)_2$-*hd*, and $(3MAI)_2$-*dd* are summarized in Table 1, together with those for the $(7AI)_2$ dimers for comparison.

The LIF spectra of $(3MAI)_2$-*hd* and $(3MAI)_2$-*dd* are very similar to those of the corresponding $(7AI)_2$ dimers.[12] The

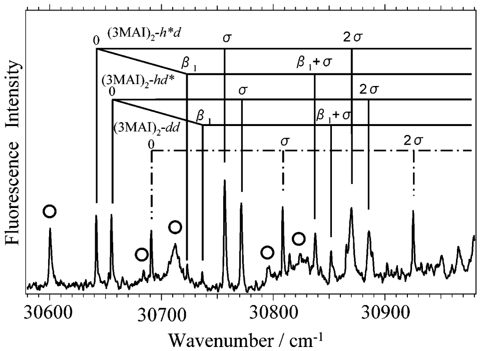

Figure 3. The LIF spectrum of a mixture of (3MAI)$_2$-*hh*, (3MAI)$_2$-*hd*, and (3MAI)$_2$-*dd* in a supersonic free jet expansion. The open circles (○) indicate vibronic bands of (3MAI)$_2$-*hh*.

TABLE 1: Wavenumbers, Bandwidths, and Assignment for Vibronic Bands in the LIF Spectra of (3MAI)$_2$ and (7AI)$_2$[a]

species	$\Delta\nu$/cm^{-1}	bandwidth/cm^{-1}	assignment
(3MAI)$_2$-*hh*	0 (30600)	3.2	origin
	84	2.7	β_1
	96		β_2
	113	10.4	σ
	196	6.8	$\beta_1+\sigma$
	209		$\beta_2+\sigma$
	225	22	2σ
	310		$\beta_1+2\sigma$
	321		$\beta_2+2\sigma$
	335		3σ
(3MAI)$_2$-*h*d*	0 (30641)	1.4	origin
	82	1.6	β_1
	115	2	σ
	196	4.2	$\beta_1+\sigma$
	228	4.5	2σ
(3MAI)$_2$-*hd**	0 (30655)	1.4	origin
	81	1.6	β_1
	116	2	σ
	197	4.8	$\beta_1+\sigma$
	230	3.4	2σ
(3MAI)$_2$-*dd**	0 (30691)	1.5	origin
	117	1.7	σ
	197		$\beta_1+\sigma$
	234	1.8	2σ
(7AI)$_2$-*hh*[b]	0 (32252)	2.7	origin
	98	2.7	β
	120	10	σ
	215		$\beta_1+\sigma$
	240		2σ
(7AI)$_2$-*h*d*[c]	0 (32293)	1.6	origin
	96	1.7	β
	121	4.1	σ
	216	2.8	$\beta+\sigma$
	239		2σ
(7AI)$_2$-*hd**[c]	0 (32314)	1.6	origin
	96		β
	123	2.4	σ
	243	5.2	2σ
(7AI)$_2$-*dd**[c]	0 (32348)		origin
	98		β
	124	2.6	σ
	222	1.7	$\beta+\sigma$
	247	2.6	2σ

[a] $\Delta\nu$ is the relative shift from the origin band. Bandwidth is full width at half-maximum (fwhm). [b] Reference 25. [c] Reference 12.

observation of a single electronic origin in the spectra of (3MAI)$_2$-*hh* and (3MAI)$_2$-*dd* implies that the degenerated zero-point levels of the dimer split into doublet states because of the excitonic interaction. The appearance of the two origins in the LIF spectrum of (3MAI)$_2$-*hd* suggests that the symmetry of the molecule changes by the deuteration of an imino hydrogen.

Two methyl groups in the (3MAI)$_2$ dimers may undergo hindered rotation. The vibronic bands due to the transition between the internal rotation states have not been observed in the LIF spectra of the three dimers, suggesting that the conformation of the two methyl groups in the lowest excited electronic state is very similar to that in the electronic ground state.

We note that a single electronic origin is observed in the LIF spectra of (3MAI)$_2$-*hh* and (3MAI)$_2$-*dd*, but the two electronic origins separated by 13 cm^{-1} are observed in (3MAI)$_2$-*hd*. This indicates that the effective symmetry of (3MAI)$_2$-*hh* and (3MAI)$_2$-*dd* belongs to the C_{2h} symmetry point group in the equilibrium structure, but that of (3MAI)$_2$-*hd* belongs to the C_s symmetry point group, where "effective" means the ignorance of the hindered rotation of the methyl group. In the optimized structure for the S_0 state of (3MAI)$_2$-*hh*, one of the CH bonds in the methyl group directs toward the $C_3{=}C_4$ double bond in the pyrrole ring. This conformation may not change upon photoexcitation to the lowest excited electronic state. Very close similarity between the vibronic patterns in the LIF spectra of the (3MAI)$_2$-*hh*, (3MAI)$_2$-*hd*, and (3MAI)$_2$-*dd* dimers[12] and those of the (3MAI)$_2$ dimers suggests that the excitation is delocalized on the two 3MAI monomer moieties in (3MAI)$_2$-*hh* and (3MAI)$_2$-*dd*, whereas that is localized on the 3MAI-*h* or 3MAI-*d* moiety in the lowest excited electronic state of (3MAI)$_2$-*hd*. The methyl substitution does not change the effective symmetry of the lowest excited state of the (7AI)$_2$-*hh* and (7AI)$_2$-*dd*. The $^1B_u \leftarrow {}^1A_g$ transition is electric-dipole allowed in (3MAI)$_2$-*hh* and (3MAI)$_2$-*dd*, but the $^2A_g \leftarrow {}^1A_g$ transition is one-photon forbidden. The symmetry of the lowest excited electronic state of (3MAI)$_2$-*h*d* and (3MAI)$_2$-*hd** belongs to the A' point group, as is the case of (7AI)$_2$-*h*d* and (7AI)$_2$-*hd**,[12] and the electronic transition to the two A' states becomes one-photon allowed. The splitting of the two electronic origins of (3MAI)$_2$-*hd* is 13 cm^{-1}, which is 8 cm^{-1} smaller than the corresponding splitting of (7AI)$_2$-*hd*.

The splitting between the ^2A_g and ^1B_u states of (7AI)$_2$-*hh* was determined to be 2 cm^{-1} by measuring the (2 + 2) resonance-enhanced multiphoton ionization spectrum.[2] The ^2A_g state is located above the ^1B_u state. The splitting between the ^2A_g and ^1B_u states of (3MAI)$_2$-*hh* is predicted to be similar to that of (7AI)$_2$-*hh*. Very recently, it was proposed by Kanamaru that the lowest excited state of (7AI)$_2$-*hh* should be treated in the weak coupling limit as Frenkel-type excitons of a L_a-type excited state;[21−23] the difference in the vibrational frequencies of the ^1B_u and ^2A_g states observed by one-photon and two-photon absorption depends on the corresponding pair of the vibronic states,[2] which cannot be explained by the strong coupling limit. The localization of the excitation on one of the monomer moieties in (7AI)$_2$-*hd* and (3MAI)$_2$-*hd* is reasonably explained by the weak coupling limit, where the vibronic states are expressed with linear combinations of the localized excited (LE) vibronic states.[21,24] In the case of (7AI)$_2$, tunneling between the two potential minima of the LE state provides a small splitting (2 cm^{-1}).[2] Because the excitonic interaction between the two monomer moieties is very weak, the introduction of a small asymmetry due to the substitution of a deuteron easily localizes the vibrational wavefunctions. We have obtained evidence of the complete localization of the vibrational wavefunctions of (7AI)$_2$-*hd* by measuring the electronic spectra of the C−H deuterated species, which will be described elsewhere.[25]

A prominent feature in the LIF spectra of the (3MAI)$_2$ dimers is a substantial change in the bandwidth depending on the vibronic state and the deuteration of the NH group. The widths of vibronic bands decrease by deuteration of an NH group, and the deuteration of two NH groups further decreases the

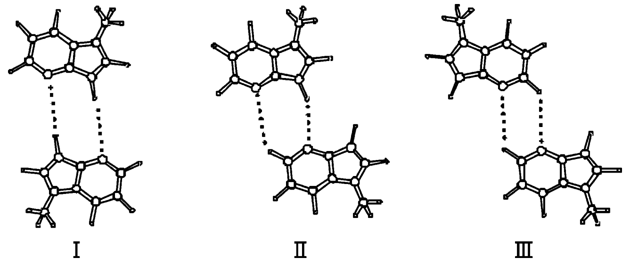

Figure 4. Structures of three isomers **I**−**III** for $(3MAI)_2$-*hh* obtained by DFT calculations at the B3LYP/cc-pVDZ level. The dotted lines (- - -) indicate the intermolecular hydrogen bond.

TABLE 2: Calculated Binding Energies (BEs)[a] for Structural Isomers of $(3MAI)_2$-*hh*

species	relative energy	BE	BSSE	BE (BSSE corrected)
isomer **I**	0.0	16.33	4.04	12.29
isomer **II**	7.63	8.70	3.46	5.24
isomer **III**	13.66	2.67	2.63	0.03

[a] In units of kcal mol^{-1}.

bandwidths. These results indicate that the three dimers undergo ESDPT, proton and deuteron transfer (ESPDT), or double deuteron transfer (ESDDT) through the tunneling mechanism. The evidence of ESPDT and ESDDT of $(7AI)_2$-*hd* and $(7AI)_2$-*dd* has been obtained by measuring the dispersed fluorescene spectra, in which fluorescence from the tautomer appears in the region of ∼24 000−32 000 cm^{-1}.[25] The dispersed fluorescence spectra of $(3MAI)_2$-*hd* and $(3MAI)_2$-*dd* may resemble those of $(7AI)_2$-*hd* and $(7AI)_2$-*dd*, although the intensity of fluorescence from $(3MAI)_2$-*hd* and $(3MAI)_2$-*dd* was too weak to obtain the dispersed fluorescence spectra.

The width of the bands (fwhm) significantly depends on the vibronic state (Table 1), indicating that vibrational-mode selective ESDPT occurs in $(3MAI)_2$-*hh*, as is also the case of $(7AI)_2$-*hh*. The intermolecular stretching mode remarkably enhances the rate for ESDPT, while the intermolecular bending mode does not enhance ESDPT. A similar vibrational-mode selective proton tunneling has been reported for tropolone[26] and 9-hydroxytropolone[27] and is attributed to the multidimensional nature of proton tunneling: The motion of the moving proton/deuteron couples with the motions of the heavy atoms that constitute the molecule and influences the tunneling path.

3.2. Effect of Methyl Substitution on ESDPT. We have carried out DFT calculations to obtain the stable structures, the binding energies, and the normal modes in the S_0 state of $(3MAI)_2$-*hh*. Three structural isomers **I**−**III** are obtained as drawn in Figure 4. Dual NH···N hydrogen-bonded isomer **I** is the most stable isomer. Isomers **II** and **III** have an NH···N and a CH···N intermolecular hydrogen bonds. The calculated binding energies for these isomers are much smaller than that for isomer **I**. The N−H and N···H hydrogen bond distances for $(3MAI)_2$-*hh* are 1.04 and 1.90 Å, respectively, while the N−H···N angle is 172.0°. The corresponding distances and the angle are the same for $(7AI)_2$ when the same basis sets are used. The BSSE corrected binding energy for the dual hydrogen-bonded isomer **I** is 5093 cm^{-1} (Table 2). The corresponding BSSE corrected binding energy for the dual hydrogen-bonded $(7AI)_2$ (5235 cm^{-1}) is 143 cm^{-1} larger than that for $(3MAI)_2$. The relative spectral shift for the origin of $(3MAI)_2$-*hh* (30 600 cm^{-1}) from the origin of 3MAI (33 432 cm^{-1}) is 2832 cm^{-1}. The corresponding spectral shift for $(7AI)_2$-*hh* is 2342 cm^{-1}. This indicates that the relative change in the binding energy upon the $S_1 \leftarrow S_0$ transition is larger than that of $(3MAI)_2$. In addition, the vibronic pattern in the LIF spectrum of $(3MAI)_2$-*hh* is very similar to that of $(7MI)_2$-*hh*. Slightly lower intermolecular stretching and bending frequencies σ and β_1 of $(3MAI)_2$-*hh* than those of $(7AI)_2$ (see Table 1) may be mainly due to the mass effect. These results imply that the shape of the ESDPT potential in the S_1 state of $(3MAI)_2$ is similar to that of $(7AI)_2$.

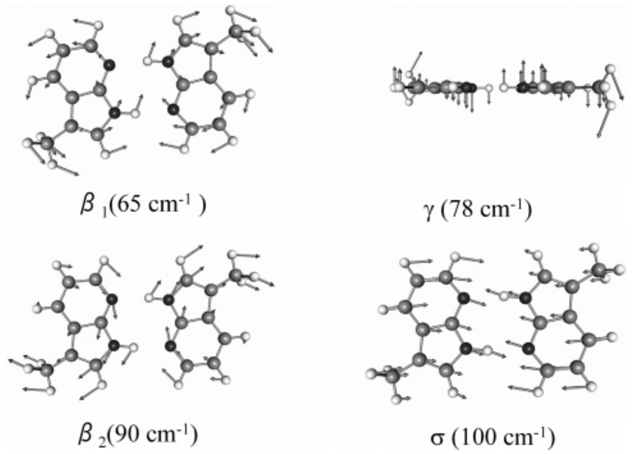
β_1(65 cm^{-1}) γ (78 cm^{-1})
β_2(90 cm^{-1}) σ (100 cm^{-1})

Figure 5. Calculated low-frequency intermolecular vibrational modes of $(3MAI)_2$-*hh* (isomer **I**). The number in the parentheses indicates the calculated frequency. No correction was made for the vibrational frequencies.

A prominent substitution effect on the intramolecular proton transfer was observed in 5-methyltropolone.[28] The substitution of a methyl group at the 5-position of tropolone substantially changes the tunneling potential because of a coupling of the internal rotation of the methyl group with the motion of the hydroxy proton. The coupling is induced by the introduction of asymmetric character to the tunneling potential of tropolone. The effect of the methyl substitution on the ESDPT reaction in $(7AI)_2$-*hh* is much smaller than our expectation. In the case of $(3MAI)_2$-*hh*, the effective symmetry of the molecules does not change by the methyl substitution. In addition, the ESDPT potential is dominated by the dual hydrogen bond. Thus, the methyl substitution provides little effect on ESDPT coordinates. However, the ESDPT potential may be influenced significantly by the substitution of an electron-donating group or an electron-withdrawing group that significantly alters the strength of the intermolecular hydrogen bonds in $(7AI)_2$.

DFT calculations provide six low-frequency intermolecular vibrations with wavenumbers 27, 36, 75, 90, 96, and 106 cm^{-1} for the S_0 state of $(3MAI)_2$-*hh* (isomer **I**). Figure 5 shows four low-frequency intermolecular vibrational modes that are candidates for the observed vibrations in the LIF spectrum (Figure 2). Two modes β_2 and σ belong to the a_g symmetry, while modes β_1 and γ belong to the b_u symmetry in the S_0 state. The transition to one quantum of γ is electric-dipole forbidden for $(3MAI)_2$ with a planar structure, but the transition to one quantum of β_1 is allowed because the lowest excited electronic state is described by a double-minimum potential well in the weak coupling limit. By comparing the experimental vibrational frequencies with the calculated ones, we assigned the three intermolecular vibrations to the fundamentals of in-plane bending vibrations β_1 and β_2 and stretching vibration σ.

3.3. LIF Spectrum of Nonreactive Dimer. The LIF spectrum in the 30 680−30 920 cm^{-1} region obtained without the Y45 glass filter is shown in Figure 6. The vibronic pattern in Figure 6 is very different from that in Figure 1, implying that fluorescence from the reactive $(3MAI)_2$-*hh* dimer is very weak. An electronic origin is observed at 30 641 cm^{-1}. The spectrum consists of two progressions with 12 and 18 cm^{-1} vibrations

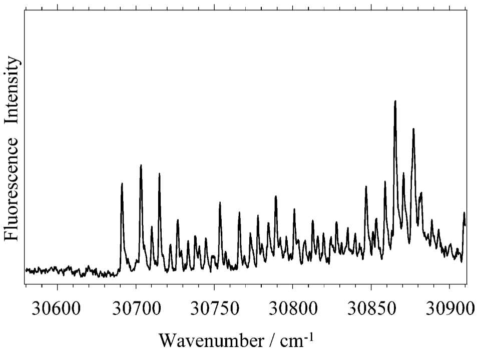

Figure 6. The LIF spectrum of the nonreactive $(3MAI)_2$ dimer measured without a Y45 glass filter (cf. Figure 2).

and progressions of the combination of the two low-frequency vibrations. This vibronic pattern in Figure 6 closely resembles that in the LIF spectrum of the nonreactive dimer of $(7AI)_2$-*hh*.[2] The IR−UV double resonance spectroscopy showed that a water molecule is hydrogen-bonded to the two 7AI moieties.[29] By analogy, the LIF spectrum in Figure 6 is ascribed to a nonreactive dimer, in which a water molecule is hydrogen-bonded to the two 3MAI moieties.

4. Conclusion

We have observed the LIF spectra of $(3MAI)_2$-*hh*, $(3MAI)_2$-*hd*, and $(3MAI)_2$-*dd* reactive dimers in a supersonic free jet expansion. Two intermolecular bending modes and a stretching mode are assigned with the aid of the normal-mode calculations. The excitonic character of the lowest excited state of $(3MAI)_2$ is explained by the weak coupling limit. The effective symmetry of the lowest excited states of $(3MAI)_2$-*hh* and $(3MAI)_2$-*dd* belongs to the C_{2h} point group because of the delocalization of the excitation on the two 3MAI moieties. In contrast, the excitation is localized on either the 3MAI-*h* or 3MAI-*d* moiety in $(3MAI)_2$-*hd*, and the separation of the origin bands of $(3MAI)_2$-*h*d* and $(3MAI)_2$-*hd** has been determined to be 13 cm^{-1}. The effective symmetry of $(3MAI)_2$-*hd* belongs to the C_s point group. The close resemblance of the vibronic pattern in the LIF spectra and the calculated binding energies for the $(3MAI)_2$ and $(7AI)_2$ reveal that the methyl substitution provides little effect on the ESDPT potential of $(7AI)_2$. The LIF spectrum of the nonreactive $(3MAI)_2$ dimer has been observed. The vibronic pattern in the spectrum is very similar to that of the nonreactive $(7AI)_2$ dimer, in which a water molecule is hydrogen-bonded to the two 7AI molecules.

Acknowledgment. This work was supported in part by the Grant-in-Aid for Scientific Research No. 15250015 from the Japanese Ministry of Education, Science, Sports and Culture.

References and Notes

(1) (a)Taylor, C. A.; El-Bayoumi, M. A.; Kasha, M. *Proc. Natl. Acad. Sci. U.S.A.* **1969**, *63*, 253. (b) Ingham, K. C.; Abu-Elgheit, M.; El-Bayoumi, M. A. *J. Am. Chem. Soc.* **1971**, *93*, 5023. (c) Ingham K. C.; El-Bayoumi, M. A. *J. Am. Chem. Soc.* **1974**, *96*, 1674.

(2) (a) Fuke, K.; Yoshiuchi, H.; Kaya, K. *J. Phys. Chem.* **1984**, *88*, 5840. (b) Fuke, K.; Kaya, K. *J. Phys. Chem.* **1989**, *93*, 614.

(3) Douhal, A.; Kim, S.; Zewail, A. H. *Nature* **1995**, *378*, 260.

(4) Douhal, A.; Guallar, V.; Moreno, M.; Lluch, J. M. *Chem. Phys. Lett.* **1996**, *256*, 370. (5) Lopez-Martens, R.; Long, P.; Sogaldi, D.; Soep, B.; Syage, J.; Millie, P. *Chem. Phys. Lett.* **1997**, *273*, 219.

(5) (a) Takeuchi, S.; Tahara, T. *Chem. Phys. Lett.* **1997**, *227*, 340. (b) Takeuchi, S.; Tahara, T. *J. Phys. Chem. A* **1998**, *102*, 7740. (c) Takeuchi, S.; Tahara, S. *Chem. Phys. Lett.* **2001**, *347*, 108.

(6) (a) Folmer, D. E.; Poth, L.; Wisniewski, E. S.; Castleman, A. W., Jr. *Chem. Phys. Lett.* **1998**, 287, 1. (b) Folmer, D. E.; Poth, L.; Wisniewski, E. S.; Castleman, A. W., Jr. *Chem. Phys. Lett.* **2000**, *318*, 637.

(7) Chachisvilis, M.; Fiebig, T.; Douhal, A.; Zewail, A. H. *J. Phys. Chem. A* **1998**, *102*, 669.

(8) Fiebig, T.; Chachisvilis, M.; Manger, M.; Zewail, A. H.; Douhal, A.; Garcia-Ochoa, I.; De la Hoz Ayuso, A. *J. Phys. Chem. A* **1999**, *103*, 7419.

(9) (a) Douhal, A.; Moleno, M.; Lluch, J. M. *Chem. Phys. Lett.* **2000**, *324*, 75. (b) Douhal, A.; Moreno, M.; Lluch, J. M. *Chem. Phys. Lett.* **2000**, *324*, 81. (c) Moreno, M.; Douhal, A.; Lluch, J. M. *J. Phys. Chem.* **2001**, *84*, 191.

(10) (a) Catalán, J.; Del Valle, J. C.; Kasha, M. *Proc. Natl. Acad. Sci. U.S.A.* **1999**, *96*, 8338. (b) Catalan, J.; Del Valle, J. C.; Kasha, M. *Chem. Phys. Lett.* **2000**, *318*, 629. (c) Del Valle, J. C.; Kasha, M.; Catalán, J. *Int. J. Quantum Chem.* **2000**, *77*, 118.

(11) Catalán, J.; Perez, P.; Del Valle, J. C.; De Paz, J. L. G.; Kasha, M. *Proc. Natl. Acad. Sci. U.S.A.* **2004**, *101*, 419.

(12) Sakota, K.; Hara, A.; Sekiya, H. *Phys. Chem. Chem. Phys.* **2004**, *6*, 32.

(13) Sekiya, H. Atom Tunneling and Molecular Structure. In *Atom Tunneling Phenomena in Physics, Chemistry and Biology*; Miyazaki, T., Ed.; Springer: Berlin, 2004.

(14) (a)Borst, D. R.; Roscioli, J. R.; Pratt, D. W.; Florio, G. M.; Zwier, T. S.; Muller, A.; Leutwyler, S. *Chem. Phys.* **2002**, *283*, 341. (b)Muller, A.; Talbot, F.; Leutwyler, S. *J. Am. Chem. Soc.* **2002**, *124*, 14486.

(15) Sobolewski, A. L.; Domcke, W. *Chem. Phys.* **2003**, *294*, 73.

(16) Chou, P. T.; Liao, J. H.; Wei, C. Y.; Yang, C. Y.; Yu, W. S.; Chou, Y. H. *J. Am. Chem. Soc.* **2000**, *122*, 986.

(17) Hung, F. T.; Hu, W. P.; Chou, P. T. *J. Phys. Chem. A* **2001**, *105*, 10475.

(18) Yu, W. S.; Cheng, C. C.; Chang, C. P.; Wu, G. R.; Hsu, C. H.; Chou, P. T. *J. Phys. Chem. A* **2002**, *106*, 8006.

(19) Robison, M. M.; Robison, B. L. *J. Am. Chem. Soc.* **1955**, *77*, 457.

(20) Frisch, M. J.; Trucks, G. W.; Schlegel, H. B.; Scuseria, G. E.; Robb, M. A.; Cheeseman, J. R.; Zakrzewski, V. G.; Montgomery, J. A., Jr.; Stratmann, R. E.; Burant, J. C.; Dapprich, S.; Millam, J. M.; Daniels, A. D.; Kudin, K. N.; Strain, M. C.; Farkas, O.; Tomasi, J.; Barone, V.; Cossi, M.; Cammi, R.; Mennucci, B.; Pomelli, C.; Adamo, C.; Clifford, S.; Ochterski, J.; Petersson, G. A.; Ayala, P. Y.; Cui, Q.; Morokuma, K.; Malick, D. K.; Rabuck, A. D.; Raghavachari, K.; Foresman, J. B.; Cioslowski, J.; Ortiz, J. V.; Stefanov, B. B.; Liu, G.; Liashenko, A.; Piskorz, P.; Komaromi, I.; Gomperts, R.; Martin, R. L.; Fox, D. J.; Keith, T.; Al-Laham, M. A.; Peng, C. Y.; Nanayakkara, A.; Gonzalez, C.; Challacombe, M.; Gill, P. M. W.; Johnson, B. G.; Chen, W.; Wong, M. W.; Andres, J. L.; Head-Gordon, M.; Replogle, E. S.; Pople, J. A. *Gaussian 98*, revision A.10; Gaussian, Inc.: Pittsburgh, PA, 1998.

(21) Kanamaru, N. *J. Mol. Spectrosc.* **2004**, *225*, 55.

(22) Davydov, A. S. *Theory of Molecular Excitons*; Plenum Press: New York, 1971.

(23) Kanamaru, N. In *Science Papers IPCR 71*; 1977, pp 85−102. Abstract-INSPEC.

(24) Southern, C. A.; Levy, D. H.; Stearns, J. A.; Florio, G. M.; Longarte, A.; Zwier, T. S. *J. Phys. Chem. A* **2004**, *108*, 4599.

(25) Sakota, K.; Sekiya, H. To be published.

(26) (a) Sekiya, H.; Nagashima, Y.; Nishimura, Y. *J. Chem. Phys.* **1990**, *92*, 5761. (b) Sekiya, H.; Nagashima, Y.; Tsuji, T.; Nishimura, Y.; Mori, A.; Takeshita, H. *J. Phys. Chem.* **1991**, *95*, 10311.

(27) Sekiya, H.; Nakano, N.; Nishi, K.; Hamabe, H.; Sawada, T.; Tashiro, M.; Nishimura, Y. *Chem. Lett.* **1995**, 893.

(28) (a)Nishi, K.; Sekiya, H.; Kawakami, H.; Mori, A.; Nishimura, Y. *J. Chem. Phys.* **1998**, *109*, 1589. (b) Nishi, K.; Sekiya, H.; Kawakami, H.; Mori, A.; Nishimura, Y. *J. Chem. Phys.* **1999**, *111*, 3961.

(29) Yokoyama, F.; Watanabe, H.; Omi, T.; Ishiuchi, S.; Fujii, M. *J. Phys. Chem. A* **2001**, *105*, 9366.